



Use of *Lentinula edodes* Extract as Corrosion Inhibitor for Carbon Steel in Sulfuric Acid

R. Suarez-Hernandez¹, G.F. Dominguez-Patiño², J.G. Gonzalez-Rodriguez¹,
I. Tello³, V.M. Salinas-Bravo⁴, J.G. Chacon-Nava⁵

¹Universidad Autónoma del Estado de Morelos, Centro de Investigaciones en Ingeniería y Ciencias Aplicadas, Ave. Universidad 1001, Chamilpa, C.P. 62209, Cuernavaca, Mor. Mexico.

²Universidad Autónoma del Estado de Morelos, Facultad de Ciencias Químicas e Ingeniería., Ave. Universidad 1001, Chamilpa, C.P. 62209, Cuernavaca, Mor. Mexico.

³Universidad Autónoma del Estado de Morelos, Facultad de Ciencias Biológicas., Ave. Universidad 1001, Chamilpa, C.P. 62209, Cuernavaca, Mor. Mexico

⁴Instituto Nacional de Electricidad y Energías Limpias, Department of Combustion, Av. Reforma 108, Temixco, Mor., Mexico

⁵Centro de Investigacion en Materiales Avanzados, Chihuahua, Mexico

Received 24 Aug 2017,
Revised 06 Apr 2018,
Accepted 20 Apr 2018

Keywords

- ✓ Corrosion;
- ✓ Green inhibitor;
- ✓ Carbonsteel;

ggonzalez@uaem.mx
Phone: +527773297084
Fax: +527773297084

Abstract

An evaluation of *Lentinula edodes* (*L. edodes*) extract as a green corrosion inhibitor for 1018 carbon steel in 0.5 M H₂SO₄ was carried out by using weight loss tests, potentiodynamic polarization curves and electrochemical impedance spectroscopy measurements. These tests were complemented by electronic microscopy analysis, infrared and UV-vis spectroscopy as well as mass chromatography. It has been found that *L. edodes* is an efficient, mixed type of inhibitor, which increases with its concentration and immersion time, but decreasing with the testing temperature. The way that *L. edodes* adsorbs on to the metal surface is chemical by following a Langmuir type of adsorption isotherm, to form protective corrosion products due to the existence of compounds, with heteroatoms such as C, O and N, in functional groups such as amine, which are the responsible for the corrosion protection

1. Introduction

Iron and its alloys are one of the most consumed metals for constructional and industrial applications [1]. However, especially in acid media, they are highly susceptible to corrosion. The employment of inhibitors is one of the most effective methods for protection of metals against corrosion [2–10]. Synthetic corrosion inhibitors are highly efficient, despite of their high operating cost and hazardous environmental effects. For these reasons, scientists have focused their research on naturally occurring, green corrosion inhibitors in recent years [11–19]. Researchers have reported several natural products as corrosion inhibitors finding that they are highly effective in protecting metals and alloys in various corrosive media. Natural products such as plants, fruits and their peels, are a great source of organic compounds and cheaper than any other synthetic chemicals. Thus, the use of natural sources of bioactive compounds is not only cost effective but also eco-friendly. Shiitake (*Lentinula edodes*) is one of the most popular mushrooms in world, with a production worldwide of around 7.5 million ton in 2000 [20]. In addition to this, *L. edodes* present antitumor, antioxidant, antimicrobial and hypocholesterolemic properties which that have been intensively investigated [21–25]. Interest in *L. edodes* is

increasing due to its high nutritional value and medicinal properties [26]. Some compounds produced by *L. edodes* such as the polysaccharide named lentinan, lentinacin, and lentysine are attributed to have antitumor, antiviral and antimicrobial properties [2-30] with no serious side effects. Additionally, it has been proved an improvement in the liver function and a reduction of viremia in patients with chronic hepatitis B [31-33] as well as an inhibition of human immunodeficiency virus infection in vitro [34] in the use of *L. edodes* extract. Thus, the goal of this research paper, is to evaluate the possibility of using *L. edodes* as a green corrosion inhibitor for 1018 carbon steel in sulfuric acid.

2. Experimental procedure

2.1 Testing solution

L. edodes was grown in the Faculty of Biology of our university and then soaked in ethanol during 20 days; after, that, all the remaining ethanol was evaporated and, finally, a fixed amount of the obtained solid paste was dissolved again in 2.5-5 mL of ethanol and used as stock solution. As corrosive solution, 0.5 M sulfuric acid (H_2SO_4) by using analytical grade reagents. Inhibitor concentrations included 0, 1, 2, 3, 4, 5 and 7 ml. Each ml of inhibitor stock solution is equivalent to 0.318 g/L according to table 1.

2.2 Testing material

For the corrosion tests, a 6.00 mm diameter rod of 1018 carbon steel was used. Specimens were encapsulated in commercial polymeric resin, ground down to 600 grade emery paper, washed and degreased with acetone. Tests were performed at room temperature, around 25 °C, 40 and 60 °C by using a water bath.

2.3 Electrochemical techniques

Employed electrochemical techniques included potentiodynamic polarization curves and electrochemical impedance spectroscopy (EIS) measurements. A conventional three-electrode glass cell with a saturated calomel and a graphite rod were used as reference and auxiliary electrodes respectively. Before starting the tests, specimens were left immersed in to the solution until the free corrosion potential value, E_{corr} , reached a steady state value, normally after 30 minutes. For the polarization curves, specimen was polarized from the cathodic to the E_{corr} value and then towards the anodic direction, starting from -1000 to +1500 mV with respect to the E_{corr} value, at a scan rate of 1 mV/s. Corrosion current density value, I_{corr} , were calculated by using Tafel extrapolation. EIS tests were performed at the E_{corr} value by applying a signal with an amplitude of 10 mV in a frequency interval of 20 KHz-0.05 Hz.

2.4 Weight loss tests

Cylindrical specimens 6.00 mm diameter and 30 mm long were cut for the weight loss tests. They were ground down to 600 grade emery paper, washed and degreased with acetone. Before and after the corrosion tests, the mass of the specimen, m_1 and m_2 , and the exposed area of the specimen, A , were measured, and, by using following equation:

$$\Delta W = (m_1 - m_2) / A \quad (1)$$

the weight loss value per unit area, ΔW , was calculated.

By knowing the weight loss without and with inhibitor, ΔW_1 and ΔW_2 respectively, Inhibitor efficiency, IE , was calculated as follows:

$$IE (\%) = 100 (\Delta W_1 - \Delta W_2) / \Delta W_1 \quad (2)$$

Selected specimens were observed in a LEO 1450VP scanning electron microscope (SEM) for their analysis.

2.5 FTIR Spectroscopic analysis

The green corrosion inhibitor as well the corrosion products were examined under FTIR analysis by using a Bruker equipment in KBr pellet in the 4500-570 cm^{-1} interval. The peak values of the FTIR were recorded. Each analysis was repeated twice to detect the characteristic peaks and their functional groups.

Table 1: Concentrations of *L. edodes* used in this work.

Volume of inhibitor stock solution (ml)	Total volume of electrolyte (ml)	Equivalent inhibitor concentration (g/L)
1	50	0.318
2	50	0.636
3	50	0.954
4	50	1.272
5	50	1.590
7	50	2.226

3. Results

3.1 Weight loss tests

A summary of the weight loss results, including, inhibitor efficiency and the metal surface coverage area, θ , for 1018 carbon steel in 0.5 M H₂SO₄ solution at different *L. edodes* concentrations and temperatures is given in table 2. It can be seen that at all different testing temperatures the weight loss decreases whereas the inhibitor efficiency value increases as the inhibitor concentration increases, reaching a highest efficiency value of 98.5% with 7 ml of inhibitor.

Table 2: Weight loss, inhibitor efficiency and surface coverage area results for 1018 carbon steel in 0.5 M H₂SO₄ in presence of *L. edodes*.

C _{inh} (ml)	ΔW (mg/cm ²)	I.E. (%)	Θ
25 °C 0	384.9	----	----
1	52.8	86	0.86
2	22	92	0.92
3	20	94	0.94
4	17	96	0.96
5	15	97.5	0.975
7	12.8	98.5	0.985
40 °C 0	470.7	----	----
1	340.9	27.6	0.276
2	274.2	41.3	0.413
3	150.6	68.2	0.682
4	75.7	83.6	0.836
5	50.5	89.5	0.895
7	32.7	94.6	0.94
60 °C 0	646.6	----	---
1	611.7	5.5	0.055
2	511	21.5	0.215
3	397.7	38.5	0.385
4	368	43.1	0.431
5	330.1	49.8	0.498
7	300.8	53.6	0.536

The surface coverage area also increases with increasing the inhibitor concentration, which indicates that the decrease in the weight loss is due to an increase in the adsorption of *L. edodes* on the steel surface. Thus, the increase in the inhibitor efficiency with increasing the inhibitor concentration can be interpreted on the basis that the adsorption amount and the coverage of inhibitor molecules increases with increasing concentration [35, 36]. When the temperature increases, the weight loss increases, obtaining the highest weight loss and the lowest

inhibitor efficiency at 60 °C indicating that the protectiveness given by the formed corrosion products decreases with an increase in the testing temperature.

In order to be sure that the corrosion inhibition is due to the inhibitor adsorption on to the steel surface, several adsorption isotherms were calculated (Temkin, Frumkin and Langmuir isotherm), but, as shown in Figure 1, the best fitting was obtained with the Langmuir type of isotherm. The Langmuir isotherm is given by:

$$C_{inh}/\theta = 1/K_{ads} + C_{inh} \quad (3)$$

Where θ is the metal surface covered by the inhibitor, given by the inhibitor efficiency divided by 100, C the inhibitor concentration and K_{ads} is the equilibrium constant of adsorption process. The K_{ads} value may be taken as a measure of the strength of the adsorption forces between the inhibitor molecules and the metal surface [37]. Large values of K_{ads} imply more efficient adsorption and hence better inhibition efficiency [38]. By using Figure1, the K_{ads} value can be calculated, which is 19.9, and the standard free energy of adsorption for the inhibitor ΔG^0 was estimated by using the equation [39]:

$$\Delta G_{ads}^0 = -RT \ln(55.5 K) \quad (4)$$

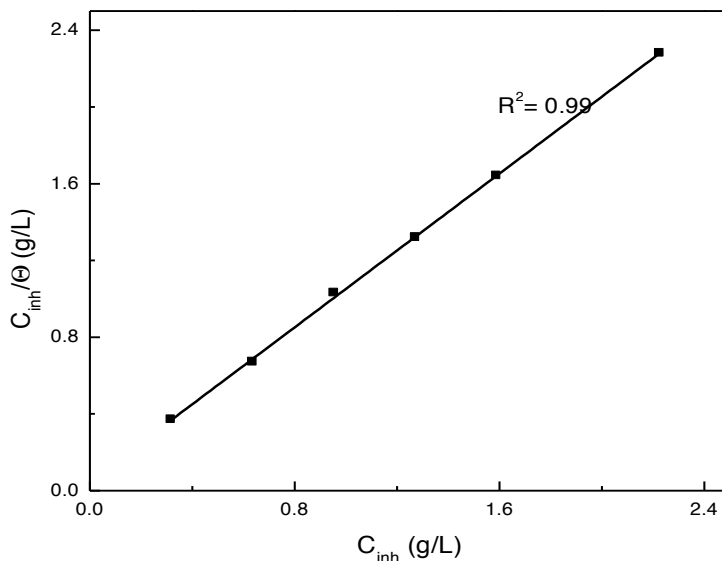
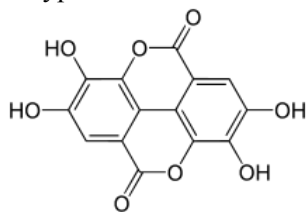


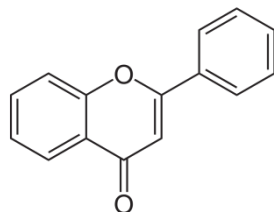
Figure 1: Langmuir adsorption isotherm obtained for 1018 carbon steel in 0.5 M H_2SO_4 in presence of *L. edodes* at 25 °C.

Since the natural extract contains infinite compounds at various percentages, we assume that the inhibition process is essentially due to the synergistic intermolecular phenomenon between molecules of natural product at major levels [40,41]. Recent works show that the ethanolic extract of *Lentinula edodes* was partially analyzed and then characterized. Polyphenols determined to be the major antioxidant component in the extract, followed by flavonoids, β -carotene and lycopene [42,43] play an essential role in inhibiting effect of corrosion process.

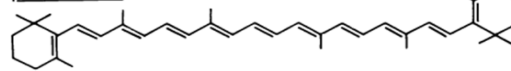
Polyphenol



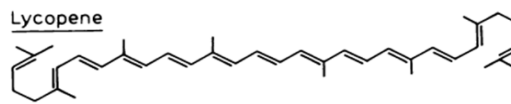
Flavonoid



β -Carotene



Lycopene



3.2 Polarization curves

Polarization curves for 1018 carbon steel in 0.5 M H₂SO₄ solution at 25 °C and different *L. edodes* concentrations is given in Figure2. For the uninhibited solution, steel display an active behavior, without evidence of formation of a passive layer. However, when *L. edodes* was added, a passive region appears for inhibitor concentrations lower than 5 ml. Electrochemical parameters are given in table 3. The E_{corr} value shifted towards more active values and the I_{corr} value decreased with the addition of *L. edodes*, reaching its lowest value with the addition of 7 ml. Inhibitor efficiency values increased with increasing the inhibitor concentration, reaching its highest value at 7 ml. Anodic Tafel slope increased when the inhibitor was added only for inhibitor concentrations lower than 5 ml, perhaps due to the presence of the passive layer, whereas the cathodic slope decreased. For inhibitor concentrations higher than 5 ml, both the anodic and cathodic Tafel slopes were very similar to those obtained in absence of the inhibitor. Thus, *L. edodes* is a mixed type of inhibitor, affecting anodic reaction with the formation of a passive, protective film at concentrations lower than 5 ml, but also affecting the cathodic hydrogen evolution reaction, maybe by a blocking effect.

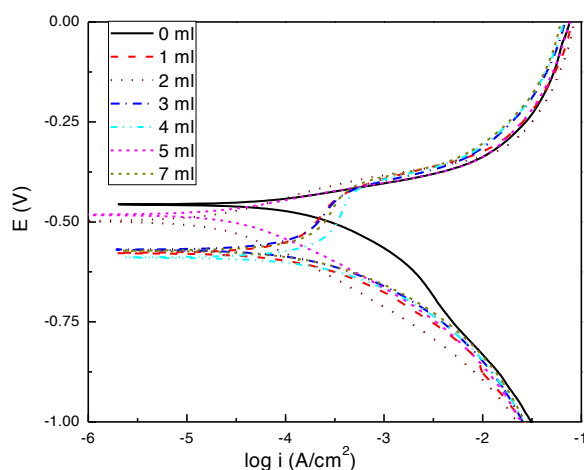


Figure 2: Effect of the polarization curves for 1018 carbon steel in 0.5 M H₂SO₄.

L. edodes concentration in

Table 3: Electrochemical parameters obtained from polarization curves for 1018 carbon steel in 0.5 M H₂SO₄ in presence of *L. edodes*.

C _{inh} (ml)	E _{corr} (V)	I _{corr} (A/cm ²)	β _a (mV/Dec)	-β _c (mV/Dec)	I _{pas} (A/cm ²)	I.E. (%)
0	-0.450	5.5E-4	40	125	----	----
1	-0.566	5.25E-4	152	108	3.5E-4	5.4
2	-0.502	4.37E-4	160	110	2.8E-4	20.4
3	-0.571	3.27E-4	170	114	2.4E-4	40.5
4	-0.583	2.63E-4	173	117	2.18E-4	52.2
5	-0.490	1.51E-4	56	135	----	72.5
7	-0.566	8.14E-5	50	130	----	85.1

3.3 Electrochemical impedance spectroscopy measurements

Nyquist plots for 1018 carbon steel in 0.5 M H₂SO₄ solution at 25 °C at different *L. edodes* concentrations is given in Figure3, where it can be seen that data describe a single loop at all the frequency values, with its center in the real axis. At low frequency values, some tails or elongations can be seen, which is due to the

accumulation or adsorption of some species at the metal/solution interface [44, 45]. The corrosion protection is given by the *L. edodes* adsorption since the diameter semicircle increases with its concentration, which indicates that the degree of metal covered by the inhibitor, θ , increases, as shown by table 1, where an increase in θ with increasing *L. edodes* concentration can be seen. Electrochemical parameters obtained from Nyquist diagrams are given in table 4. In this table, R_s is the solution resistance, R_{ct} the charge transfer resistance, and C_{dl} the double layer capacitance. It can be seen from this table that R_{ct} increases whereas the double layer capacitance value, C_{dl} , decreases with an increase in the *L. edodes* concentration due to the adsorption of *L. edodes*.

In addition, the values of the double-layer capacitance (C_{dl}) decrease by adding inhibitor in to corrosive solution. An alternative way to calculate double-layer capacitance is:

$$C_{dl} = \epsilon \epsilon_0 A / \delta \quad (5)$$

where ϵ is the double layer dielectric constant, ϵ_0 the vacuum electrical permittivity, δ the double layer thickness, and A the surface area. Thus, the decrease in the C_{dl} value is due to the replacement

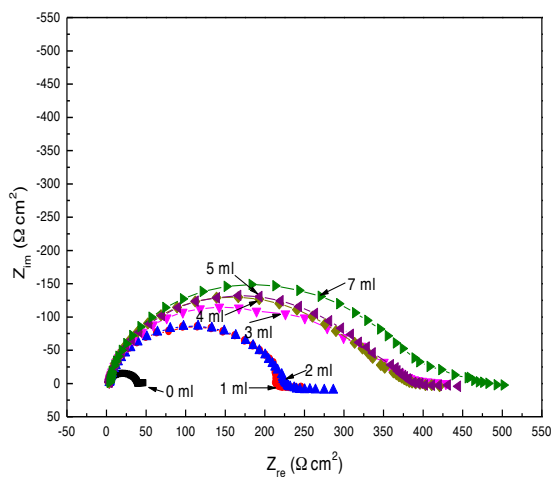


Figure 3: Effect of *L. edodes* concentration in the Nyquist diagrams for 1018 carbon steel in 0.5 M H_2SO_4 .

of water molecules at the surface metal, which have lower dielectric constant, by the inhibitor [47-48]. This point suggest that the role of inhibitor molecules is preceded by its adsorption at the metal–solution interface.

Table 4: Electrochemical parameters obtained from Nyquist diagrams curves for 1018 carbon steel in 0.5 M H_2SO_4 in presence of *L. edodes*.

$C_{inh}(ml)$	$R_s (\Omega cm^2)$	$R_{ct} (\Omega cm^2)$	$C_{dl} (\mu F cm^{-2})$	I.E. %
0	3.60	37	3.46E-05	---
1	3.71	218	2.31E-05	83.25
2	4.16	225	2.24E-05	83.79
3	3.81	382	1.67E-05	90.60
4	3.67	388	1.60E-05	90.43
5	4.23	395	1.31E-05	90.76
7	4.27	402	1.12E-05	90.91

Since the corrosion protection is given by the film formed by *L. edodes* on to the steel surface, the time that this film remains on the surface was evaluated by carrying out some EIS measurements during long periods of time without and with 7 ml of *L. edodes*. Evolution of Nyquist diagrams for both uninhibited solution are

shown in Figure. 4, whereas that for the solution containing 7 ml of *L. edodes* is given in Figure 5. It can be seen that, at all testing times, data display a capacitive loop at all frequency values. The presence of a single loop regardless of the testing time, indicates that the corrosion process is under charge transfer control and it does not change with time. For the uninhibited solution, the loop diameter increases only during the first 3 hours, and decreases after that time, whereas for the solution containing 7 ml of *L. edodes*, the loop diameter increases monotonically as time increases, for times as long as 144h, indicating that the *L. edodes* adsorption increases with time. For times longer than 144 h, the semicircle diameter decreases, indicating the desorption of *L. edodes* from the steel surface.

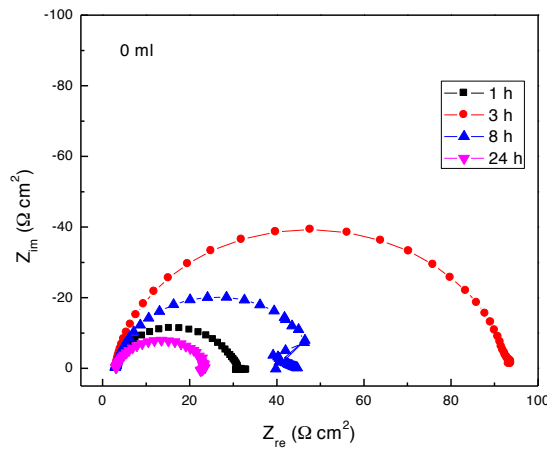


Figure 4: Nyquist diagrams at different exposure times for 1018 carbon steel in uninhibited 0.5 M H₂SO₄ solution.

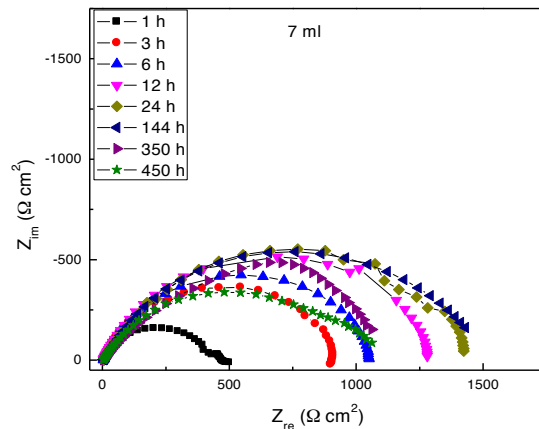


Figure 5: Nyquist diagrams at different exposure times for 1018 carbon steel in 0.5 M H₂SO₄ solution containing 7 ml of *L. edodes*.

3.4 SEM images

Some SEM micrographs of specimens corroded in absence and presence of *L. edodes* are shown in Figure 6. For specimens corroded without addition of *L. edodes*, Figure 6 a, c and e, the corrosion products formed film present a big amount of porous and micro cracks, which allow the corrosive solution to penetrate the film and corrode the underlying metal. As the temperature increases, the number of defects such as micro cracks increase, making less protective the formed film. On the other hand, for the specimens corroded in presence of 7 ml of *L. edodes*, Figure 6 b, d and f, the formed film on top of the steel surface is much more compact than that

formed in the uninhibited solution, without defects such as porous and micro cracks, which makes the film to be more protective against the ingress of the corrosive solution.

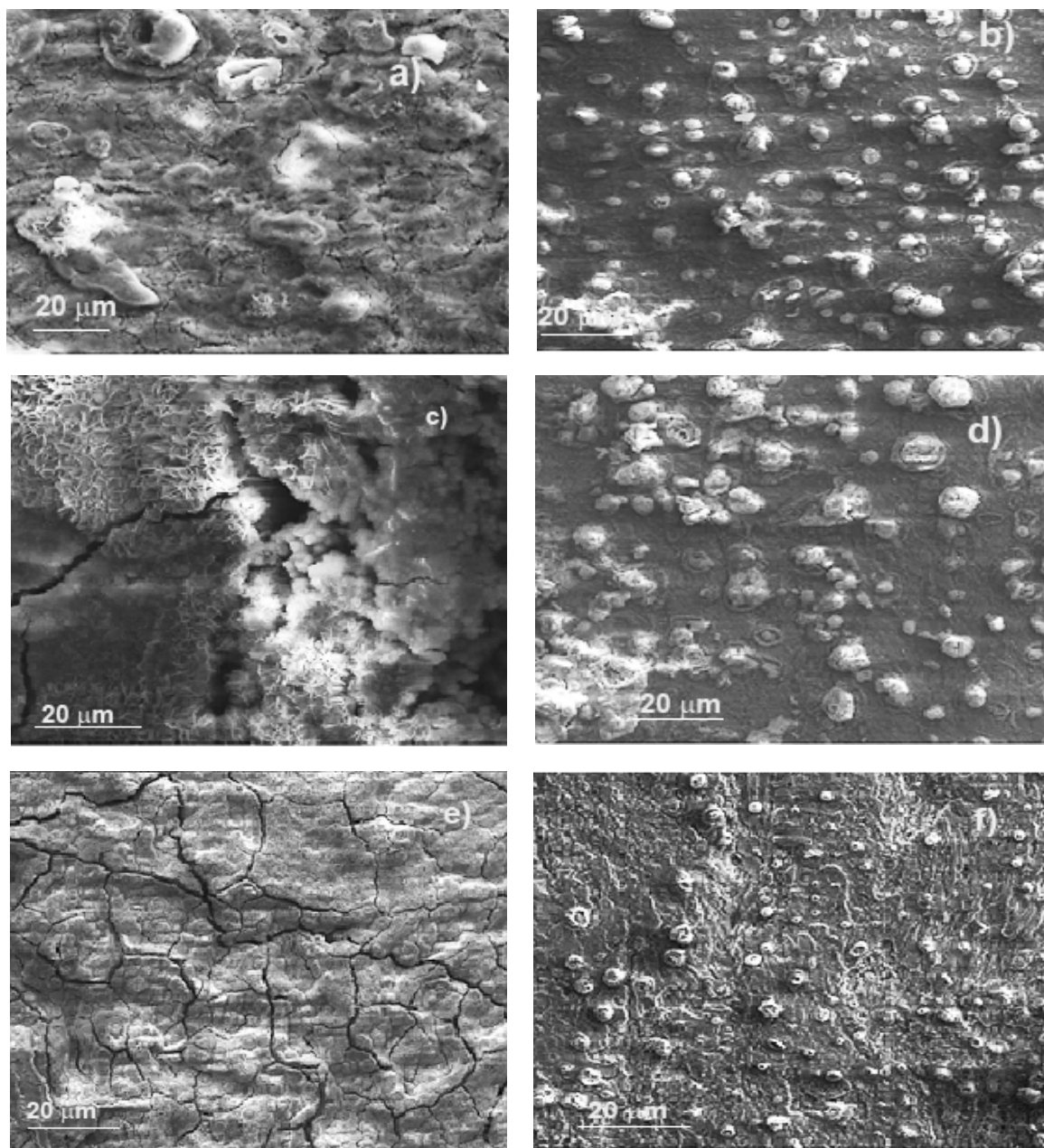


Figure 6: SEM micrographs of 1018 carbon steel samples corroded at 25 °C, a) and b), 40 °C, c) and d) and 60 °C, e) and f) containing 0 ml, a), c) and e) and 7 ml, b), d) and f) of *L. edodes*.

3.6 Infrared Spectroscopy.

FTIR spectrum for *L. edodes* extract is shown in Figure 7, where a typical signal of the O-H link, which is known to passivate metals, can be seen at 3382 cm^{-1} , whereas a strong signal at 2978 cm^{-1} is observed which corresponds to the N-H links, very likely to the amine group; another signal can be seen at 2900 cm^{-1} corresponds to the methyl, $-\text{CH}_3$, group, whereas a strong signal at 1643 cm^{-1} is for the C-O link, which is evidence of the presence of carboxylic acid. On the other hand, observed signal at 1390 cm^{-1} corresponds to the vibrations for the C-C link, characteristic for aromatic rings, and the signal at 1046 cm^{-1} has been assigned to the

C-N group, whereas the signal observed at 872 cm^{-1} corresponds to the vibrations of the C-H group. On the other hand, FTIR spectrum for the corrosion products formed on 1018 carbon steel exposed to $0.5\text{ M H}_2\text{SO}_4 + 7\text{ ml}$ of *L. edodes* is given in Figure 8, where the presence of the N-H link, from the amine group and that for the C-N group can be observed at 2978 and 1046 cm^{-1} respectively, same functional groups found in the pure *L. edodes* extract. The signal observed at 469 cm^{-1} corresponding to the vibration of the Fe-O group, is very likely to correspond to the iron oxides formed on to the steel surface. Thus, this is an evidence that the amine group present in the amino acids, is one of themain responsible for the corrosion protection given by *L. edodes* to 1018carbon steel in sulfuric acid. The $[\text{Fe-L. edodes}]$ complex may be a stable complex adsorbed on the steel surface, forming covalent or coordinate bonds between the anionic components of *L. edodes* extract and vacant Fe d-orbital. The metal/inhibitor bond usually leads to corrosion inhibition through adsorption [51]. Also, the functional groups of the formed complex by released Fe^{2+} ions and *L. edodes* extract may be soluble leading to a catalytic effect, thus accelerating corrosion, as shown in table 2 at 40 and $60\text{ }^\circ\text{C}$. The plant extract biomass is composed of many chemical compounds with a probability of both mechanisms operating concurrently. The inhibiting effect of *L. edodes* can be attributed to the resultant effect of both corrosion accelerating and retarding mechanisms. The corrosion retarding mechanism through stable complex formation dominates at increasing concentration till a critical concentration is reached where formation of soluble complex dominates. This trend has been previously reported [52].

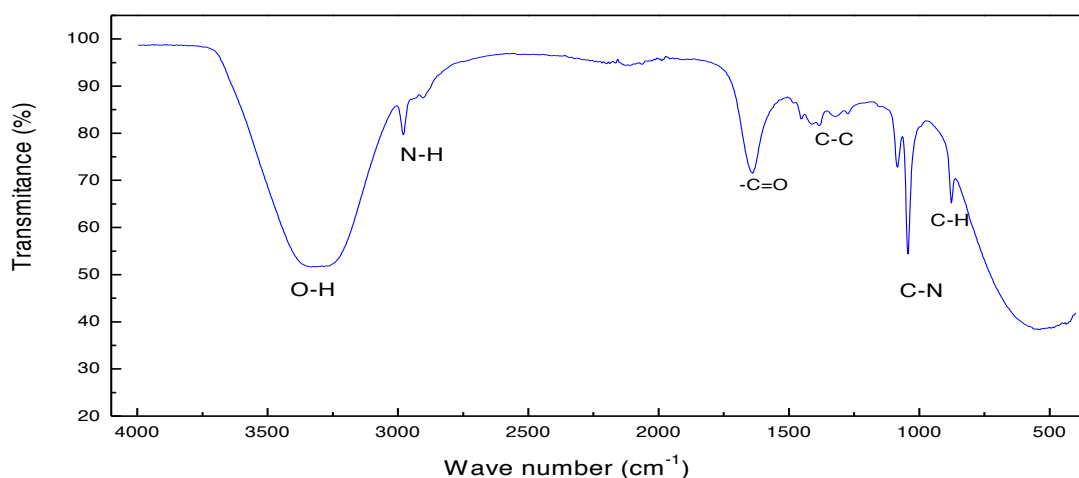


Figure 7: FTIR spectrum of pure *L. edodes* extract.

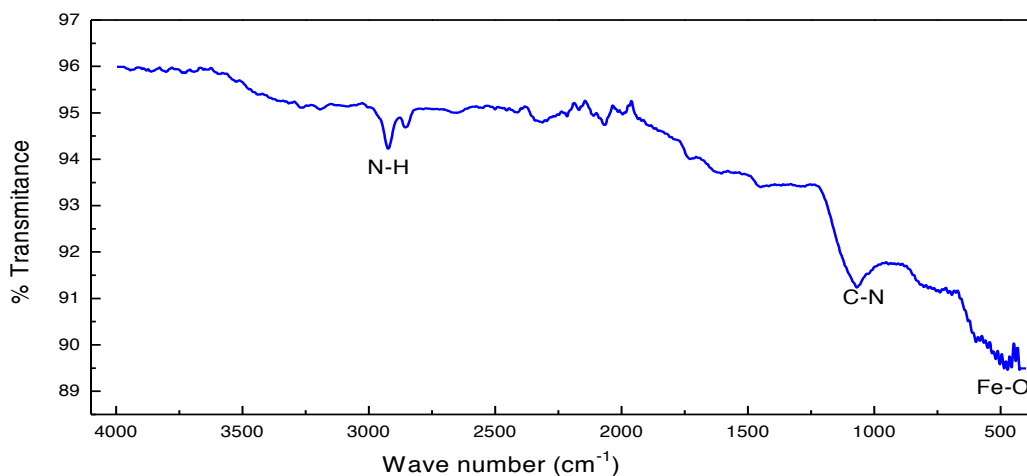


Figure 8: FTIR spectrum of corrosion products formed on top of 1018 carbon steel corroded in 0.5 M H₂SO₄ solution containing 7 ml of *L. edodes*.

Conclusions

An evaluation of *L. edodes* as a green corrosion inhibitor for 1018 carbon steel in 0.5 M H₂SO₄ has been carried out. It was found that *L. edodes* is a good corrosion inhibitor with an efficiency increasing with its concentration and exposure time, but it decreases with an increase in the temperature. *L. edodes* acts as a mixed type of inhibitor, which adsorbs chemically on to the steel by following a Langmuir type of adsorption isotherm to form a protective corrosion products layer on the steel. This protection is given due to the existence of compounds which contain heteroatoms such as C, N and O, present in the amino acids, forming covalent or coordinate bonds between the anionic components of *L. edodes* extract and vacant Fe d-orbital.

Acknowledgments: The authors would like to thank PRODEP for their financial support to carry out this project.

References

1. R. Bansal, J. K. Singh, V. Singh, D. D. N. Singh, P. Das, *J. Mat. Eng. Perf.* 26 (2017) 969-977.
2. A. E. Somersa, B. R.W. Hintona, C. de Bruin-Dickason, G. B. Deacon, P. C. Junk, M. Forsyth, *Corros. Sci.* 139 (2018) 430-437.
3. Y. Qiang, S. Zhang, S. Yan, X. Zou, S. Chen, *Corros. Sci.* 126 (2017) 295-304.
4. L. Feng, S. Zhang, Y. Qiang, S. Xu, B. Tan, S. Chen, *Mater. Chem. Phys.* 215 (2018) 229-241.
5. M. Lashgari, A.M. Malek, *Electrochim. Acta* 55 (2010) 5253-5262.
6. G. Babaladimath, V. Badalamoole, S.T. Nandibewoor, *Mater. Chem. Phys.* 205 (2018) 171-179.
7. M.A. Chidiebere, E.E. Oguzie, L. Liu, Y. Li, F. Wang, *J. Ind. Eng. Chem.* 26 (2015) 182-192.
8. K. Chatoui, S. Echih, H. Harhar, A. Zarrouk, M. Tabyaoui, *J. Mater. Environ. Sci.* 9 (2018) 1212-1223.
9. G.A. Zhang, Y.F. Cheng, *Corros. Sci.* 127 (2017) 87-94.
10. H. Tian, Y.F. Cheng, *Corrosion* 72 (2016) 472-485.
11. D. Gingasu, I. Mindru, O. C. Mocioiu, S. Preda, *Mater. Chem. Phys.* 182 (2016) 230-239.
12. M.P. Desimonea, G. Grundmeier, G. Gordillo, S.N. Simison, *Electrochim. Acta* 56 (2011) 2990-2998.
13. A.S. Fouda, G. El-Ewady Ali, *Green Chem. Let. Rev.* 10 (2017) 88-100.
14. R. Haldhar, D. Prasad, A. Saxena, *J. Env. Chem. Eng.* 6 (2018) 2290-2301.
15. F. Ebich, R. Ramdan, M. Saadouni, Y. El Aoufir, A. Chaouiki, S. Ska, A. Zarrouk H. Oudda, A. Essamri, *J. Mater. Environ. Sci.* 9 (2018) 1779-1786.
16. Y. Qiang, S. Zhang, L. Guo, X. Zheng, B. Xiang, S. Chen, *Corros. Sci.* 119 (2017) 68-78.
17. A.S. Abbas, É. Fazakas, T.I. Török, *Int. J. Corros. Scale Inhib.* 7 (2018) 38-47.
18. G. Babaladimath, V. Badalamoole, S.T. Nandibewoor, *Mater. Chem. Phys.* 205 (2018) 171-179.
19. E. Alibakhshi, M. Ramezanzadeh, G. Bahlakeh, B. Ramezanzadeh, M. Mahdavian, M. Motamedi, *J. Mol. Liquids* 255 (2018) 185-198.
20. J.L. Rios, M.C. Recio, A. Viller, *J. Ethnopharmacol.* 23 (1988) 127-134.
21. N. Hatvani, *Int. J. Antimic. Ag.* 17 (2001) 71-78.
22. P. Manzi, L. Pizzoferatto, *Food Chem.*, 68 (2000) 315-322.
23. J. L. Mau, G.R. Chao, K.T. Wu, *J. Agric. Food Chem.* 49 (2001) 5461-5470.
24. Y. Shimada, T. Morita, K. Sugiyama, *J. Nutr.* 3 (2003) 758-767.
25. J.H. Yang, H.C. Lin, J.L. Mau, *Food Chem.* 77 (2002) 229-236.
26. Y.Y. Maeda, S. Takahama, H. Yonekawa, *Immunogenetics* 47 (1998) 159-171.
27. M.L. Ng, A.T. Yap, *J. Alternative Complem. Med.* 56 (2002) 581-590.
28. P.H. Ngai, T.B. Ng, *Life Sci.*, 73 (2003) 363-372.
29. S. Komemushi, Y. Yamamoto, T. Fujita, *J. Antibac. Antifung. Agents* 23 (1995) 81-90.
30. S. Komemushi, Y. Yamamoto, T.T. Fujita, *J. Antibac. Antifung. Agents* 24 (1996) 21-30.
31. G. Chihara, J. Hamuro, Y. Maeda, Y. Arai, F. Fukuoka, *Cancer Res.* 30 (1970) 2776-2787.

32. N. Sugano, Y. Hibino, Y. Choji, H. Maeda, *Cancer Lett.* 17 (1982) 109-112.
33. H. Amagas, *Princeton: Exerpta Medica* 45(1987) 316-325.
34. T.S. Tochikura, H. Nakashima, Y. Ohashi, N. Yamamoto, *Med. Microbiol. Immunol.* 177 (1988) 235-244.
35. K. Rahmouni, M. Keddou, A. Srhiri, H. Takenouti, *Corros. Sci.* 47 (2005) 3249-3265.
36. L. Boussemlil, C. Fiaud, B. Tribollet, E. Triki, *Electrochim. Acta* 44(1999) 43574367.
37. I. Kowalska, A. Stochmal, I. Kapusta, B. Janda, C. Pizza, S. Piacente, W. Oleszek, *J. Agric. Food Chem.*, 55 (2007) 2645-2654.
38. A. Stochmal, W. Oleszek, *J. Food Agric. Env.* 5 (2007) 170-179.
39. R.A. Dixon, C.L. Steele, *Trends in Plant Science* 4 (1999) 394-404.
40. S. Andreani, M. Znini, J. Paolini, L. Majidi, B. Hammouti, J. Costa, A. Muselli, *J. Mater. Environ. Sci.* 7 (2016) 187-195
41. A. Khadraoui, A. Khelifa, K. Hachama, H. Boutoumi, B. Hammouti, *Chem. Engin. Commun.* 203 (2016) 270-277
42. E.J. Choi, Z.Y. Park, E.K. Kim, *Molecules.* 21 (2016) E993. doi: [10.3390/molecules21080993](https://doi.org/10.3390/molecules21080993)
43. C. Sánchez, Bioactives from mushroom and their application. *Food bioactives*, Cham: Springer International Publishing. eBook ISBN 978-3-319-51639-4 (2017) 23–57. http://dx.doi.org/10.1007/978-3-319-51639-4_2
44. M. Özcan, İ. Dehri, M. Erbil, *Appl. Surf. Sci.* 236 (2004) 155-167.
45. R. Solmaz, G. Kardas, M. Culha, B. Yazıcı, *Electrochim. Acta* 53 (2008) 5941-5956.
46. A.K. Singh, M.A. Quraishi, *Corros. Sci.* 52 (2010) 152-170.
47. E. Poorqasemi, O. Abootalebi, M. Peikari, F. Haqdar, *Corros. Sci.* 51 (2009) 1043-1062.
48. T. Poornima, J. Nayak, A.N. Shetty, *J. Appl. Electrochem.* 41 (2011) 223-230.
49. M. Sangeetha, S. Rajendran, J. Sathiyabama, *Portug. Electrochim. Acta* 29 (2011) 429-438.
50. N. Caglarirmak, *Food Chem.* 105 (2007) 1188-1198.
51. O. Benali, H. Benmehdi, O. Hasnaoui, C. Selles, R. Salghi, *J. Mater. Env. Sci.* 4 (2013) 127-136.
52. A.M. Abdel-Gaber, B.A. Abd-El-Nabey, I.M. Sidahmed, A.M. El-Zayady, M. Saadawy, *Corros. Sci.* 48 (2006) 2765-2782.

(2018) ; <http://www.jmaterenvirosci.com>